# QCD AT LEP

**J. William Gary**
**Physikalisches Institut der Universität**
**D-6900 Heidelberg, FRG**

**Abstract**

The large data samples, high center-of-mass energy and clean environment of the $e^+e^-$ collider LEP, at CERN, allow tests of QCD to be performed with unprecedented precision. A discussion and selected review of experimental results from the first year and one half of LEP operation is given.

Table 1: Published QCD results from the LEP experiments; the symbol + means that the analysis was performed outside a collaboration, using the experiment's published data.

| | ALEPH | DELPHI | L3 | OPAL |
|---|---|---|---|---|
| Jet Production Rates | | X | X | X |
| Gluon Self-coupling | | X | X | X |
| $\alpha_S$ from: jet rates | X | X | X | X |
| event shapes | X | | | + |
| energy correlations | X | X | X | X |
| Soft Gluon Coherence | | | X | X |
| String Effect | | | | X |
| Intermittency | | X | | X |
| Charged Multiplicity Distribution | | X | | |
| Global Event Shapes | X | X | | X |
| Particle Inclusive Distributions | X | X | X | X |

## Introduction

LEP offers many advantages relative to previous $e^+e^-$ colliders for the study of Quantum Chromodynamics (QCD). The large cross section for producing hadronic final-states on the $Z^0$ resonance has yielded, in the first year and a half of LEP operation, data samples of 120,000-180,000 events for each experiment: these equal or exceed the data samples collected by the PEP or PETRA experiments during their entire lifetimes. The larger center-of-mass energy of LEP means that theoretical uncertainties are smaller than for previous studies, because uncalculated higher order terms are less important due to the smaller value of the strong coupling constant $\alpha_S$. The uncertainty from hadronization, the as-yet uncalculable process by which partons become confined inside hadrons, is also smaller for LEP's larger c.m. energy since hadronization is associated with a fixed energy scale – that of the hadron masses – so that its relative contribution to the value of a measured quantity falls like $1/E_{c.m.}$. Lastly, the LEP detectors are more sophisticated and cover a larger solid angle than detectors at previous $e^+e^-$ facilities. Therefore the LEP data permit tests of QCD with unprecedented precision. The large data samples and smaller theoretical errors make tests of QCD possible, which differ qualitatively from what was possible before.

A summary of published QCD results from LEP is given in table 1. from the four experiments ALEPH, DELPHI, L3 and OPAL. An impressive total of approximately 30 papers have appeared in about one year. The topics can be divided into those related to short distance interactions of quarks and gluons, to long distance interactions or to both. Topics related to short distances are, in general, tests of exact matrix element formulae: these include studies of jet production rates and tests for the existence of the triple gluon vertex. The evaluation of the magnitude of $\alpha_S$ at the $Z^0$ peak has been a major activity at LEP and also falls into this category. Topics related to long distances include soft gluon coherence and the so-called string effect. These test analytic formulae based on the Modified Leading Logarithm (MLLA) formulation of perturbation theory. Other, more general studies of hadronic final-states include intermittency, which is a method to examine non-statistical fluctuations in particle production, and the charged particle multiplicity distribution: these test the QCD parton cascade framework, from a statistical viewpoint. Studies of global event shapes and inclusive particle distributions are related to both short and long distance interactions because they are sensitive to hard, acolinear gluon radiation, to internal jet structure and to details of hadronization.

In the following, selected results from QCD at LEP are discussed. Emphasis is placed on results which illustrate the character or diversity of these studies. Both published and preliminary material are used for this discussion.

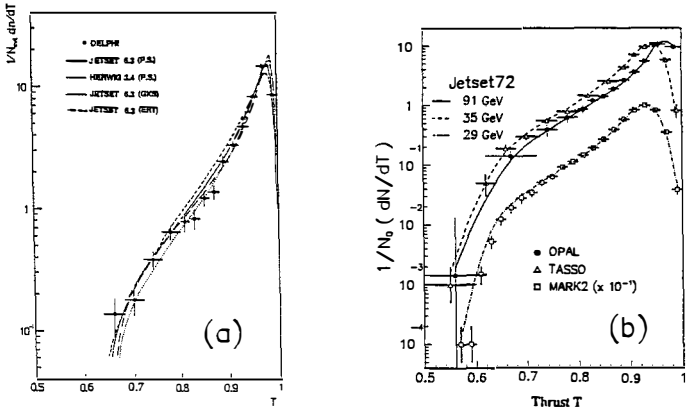


Figure 1: Thrust distribution from (a) DELPHI [1] and (b) OPAL [5].

## Event Shapes

Figure 1 (a) shows an example of a global hadronic event shape measurement from LEP, in this case the published Thrust distribution from DELPHI [1]. Thrust $T$ [2], defined by

$$T = max \left( \frac{\sum_i |\vec{p}_i \cdot \hat{n}|}{\sum_i |\vec{p}_i|} \right) \quad ; \quad \hat{n} \equiv \text{thrust direction} \tag{1}$$

is the best known shape variable used in $e^+e^-$ annihilations. The sums in (1) run over the particle momentum 3-vectors $\vec{p}$ in an event. Shown in comparison to the DELPHI data are the predictions from several QCD Monte Carlo programs which simulate perturbative QCD and parton hadronization: (a) The Jetset Monte Carlo [3] with a cascade of quarks and gluons (parton shower) followed by Lund string fragmentation, (b) the Jetset Monte Carlo with 2nd order matrix elements followed by Lund string fragmentation and (c) the Herwig Monte Carlo [4] with a parton shower followed by Wolfram-type cluster fragmentation. The model parameters have been tuned to describe multihadronic distributions from PEP and PETRA and in all cases describe the basic features of the LEP data quite well.

Figure 1 (b) shows the Thrust distribution from OPAL [5]. The distribution from Jetset with a parton shower is shown in comparison. In this case, the model parameters have been tuned to the $Z^0$ data and a very good description is obtained. The model parameters as optimized for LEP also yield very good descriptions of the Thrust measurements from PEP and PETRA, as shown. Figure 2 (a) shows how the mean of $< 1 - T >$ changes from PEP/PETRA to LEP, according to this same Jetset model, at the parton and hadron levels. The decrease in the parton level curve as $E_{c.m.}$ increases is due to the smaller rate for hard acolinear gluon radiation for the larger energy, related to the smaller value of $\alpha_S$: this is therefore a scaling violation. The energy evolution of the Thrust distribution is well described by this scaling violation in conjunction with the energy independent parameterization for the hadronization, as seen from figure 1 (b).

The correction required for hadronization, that is the factor which relates the experimental measurements to theoretical calculations, is given by the ratio of the hadron to the parton level distributions. The hadronization correction for $< 1 - T >$ is shown in figure 2 (b) for Jetset (with a parton shower) and Herwig. The hadronization correction decreases with the inverse

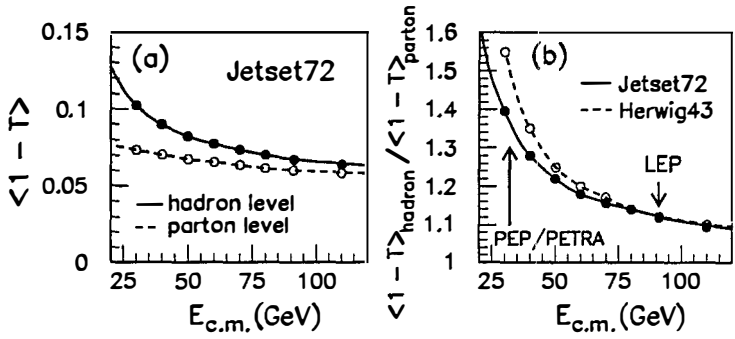


Figure 2: Evolution of (a) $< 1 - T >$ and (b) its hadronization correction with c.m. energy.

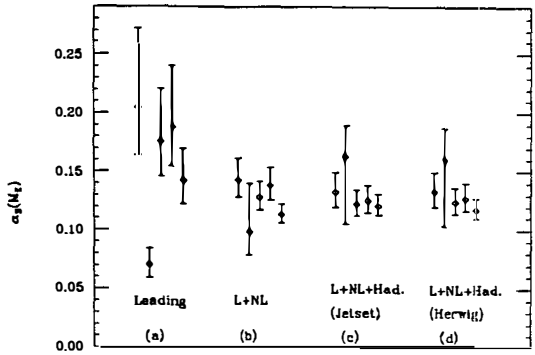


Figure 3: $\alpha_S$ measurements from event shapes [6].

of c.m. energy, as expected. At PEP and PETRA energies of about $E_{c.m.} \approx 30$ GeV, the hadronization correction is 40-50%. There is some disagreement between Jetset and Herwig as to its magnitude. At LEP the hadronization correction is about 10% and the different models agree well with each other. This is a key feature of QCD at LEP: the small hadronization correction and its well understood nature allow experiment and theory to be compared in a more direct and unambiguous way than was previously the case.

A specific example is given by the $\alpha_S$ analysis of Magnoli, Nason and Rattazzi [6], which uses the event shape variables Thrust, Oblateness, Thrust major and the C parameter measured by OPAL. The definitions of these variables are given in [5]. The measured 3-jet event rate from OPAL [7] is included as a fifth variable. The results of this analysis are shown in figure 3. The leftmost group of data points, labeled (a), shows the values of $\alpha_S$ which are extracted using leading order (tree level) calculations: the five $\alpha_S$ measurements are not consistent with each other. The group of data points labeled (b) in figure 3 shows the corresponding result when the full 2nd order theory is used. The five measurements in this case are in much better agreement. For (a) and (b), the theoretical calculations are compared directly to the experimental measurements, with no hadronization correction. The results obtained from the full 2nd order theory if a hadronization correction from either Jetset or Herwig is applied are shown in (c) and (d): the five $\alpha_S$ values come into better agreement yet. Comparing (a) to

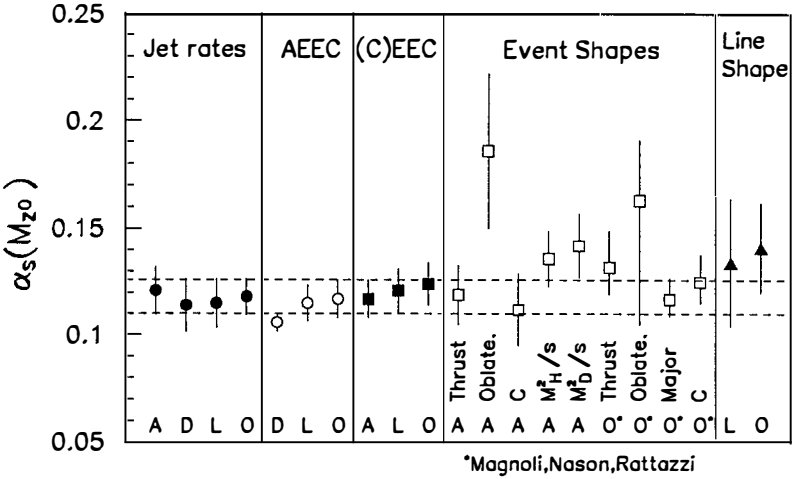


Figure 4: Published $\alpha_S$ measurements from LEP. The experiments ALEPH, DELPHI, L3 and OPAL are designated by their first initial. The dashed lines show the $1\,\sigma$ limits for a weighted average [8].

(b), it is seen that the next-to-leading-order theoretical correction is more important than the hadronization one: the effect of this latter correction is seen by comparing (b) to either (c) or to (d). Figure 3 thus illustrates that the hadronization correction at LEP is small enough that QCD radiative corrections can be tested directly and that the hadronization corrections from the model calculations provide sensible results which can be trusted, for the $Z^0$ energy.

## $\alpha_S$ Measurements

A summary of the published $\alpha_S$ measurements from LEP is given in figure 4. All are based on comparison of data to 2nd order calculations. Four general classes of variables are employed: (1) jet rates, (2) energy correlations, (3) event shapes and (4) the $Z^0$ line shape and forward-backward asymmetry. The most precise measurements come from jet rates and the energy-energy correlation asymmetry (AEEC). Measurements of $\alpha_S$ from fits to the $Z^0$ line shape and forward-backward asymmetry have larger errors but represent the only category which is still limited by statistics: in the future the $Z^0$ line shape could yield the most precise value of $\alpha_S$ at the $Z^0$ peak, as more data are accumulated, because the experimental and theoretical errors for this method are believed to be small compared to the other methods. Since the $\alpha_S$ measurements shown in figure 4 are, in general, limited by systematic errors, their combination into a weighted average requires subjectivity. A recent estimate [8] yields $\alpha_S = 0.118 \pm 0.008$ as a combined result from LEP: thus $\alpha_S$ is presently measured with about 7% precision. The one standard deviation limits from this combined result are shown by the dashed lines in figure 4. Most of the $\alpha_S$ measurements lie within these bounds. None differ by more than two standard deviations as given by the error of an individual measurement.

The relatively small scatter between the $\alpha_S$ values in figure 4 implies that the different measurements may not be completely independent. Common features between the analyses are easy to identify: most rely on the same models to obtain a hadronization correction and (in some cases) to correct for the absence of higher than 2nd order terms in the theory. The same 2nd order formulae are often used: those of [9] are especially popular.

Table 2: Comparison of energy-energy correlation analyses at LEP. The error from the dependence on renormalization scale is not included; $Q_0$ is the parton virtuality scale.

| | ALEPH | L3 | OPAL |
|---|---|---|---|
| Event Sample | 106,000 | 83,000 | 70,000 |
| Particle Sample | Charged tracks | EM + Hadronic clusters | Charged tracks + EM clusters |
| Data Handling | Cluster EEC; ($y_{cut}$) | Particle EEC; Correct to parton level ($Q_0 = 16$ GeV) | Particle EEC; Correct to parton level ($Q_0 = 1$ GeV) |
| Theory Handling | ERT (KN) Correct CEEC to to hadron level | ERT (KN) (check other theories) | ERT (KN) (check other theories) |
| $\alpha_S =$ | $0.118 \pm 0.005$ | $0.121 \pm 0.004$ | $0.124 \pm 0.006$ |

As an example, the measurement of $\alpha_S$ from the energy-energy correlation function EEC [10] is instructive. Analyses of EEC have been presented by ALEPH [11], L3 [12] and OPAL [13]: these analyses are compared in table 2. The EEC function is defined by

$$EEC(\chi) = \frac{1}{\Delta\chi \cdot N} \int_{\chi - \frac{\Delta\chi}{2}}^{\chi + \frac{\Delta\chi}{2}} \sum_{events}^{N} \sum_{i,j} \frac{E_i E_j}{E_{vis}^2} \delta(\chi' - \chi_{ij})\, d\chi' \quad ; \quad \Delta\chi = \text{bin width} \qquad (2)$$

where $N$ is the number of events; the visible event energy $E_{vis}$ is given by the sum over the particle energies. For OPAL and L3, $\chi_{ij}$ is the angle between two particles $i$ and $j$ in an event, which have energies $E_i$ and $E_j$. For ALEPH $i$ and $j$ refer to jets instead of particles: they call their method "cluster EEC" or CEEC. The jets for the ALEPH analysis are identified using the $E0$ scheme of jet recombination [9]: as a consequence the CEEC has particularly small hadronization corrections. The OPAL and ALEPH results for $\alpha_S$, shown in table 2, differ by $1\,\sigma$; the L3 result lies in between. The errors quoted here include the uncertainties from the experiment, the hadronization correction and missing higher order terms. Since these effects are treated in quite different manners by the 3 experiments, as outlined in table 2, the 3 results may be considered to be basically independent: the errors are dominated by systematic effects and so the different measurements should not differ by more than about $1\,\sigma$ if the error evaluations are correct. An additional error, of theoretical origin, needs to be included for the final result: that associated with the choice of the renormalization scale. The choice of renormalization scale is found to have an important effect on the value of $\alpha_S$ extracted from EEC: inclusion of this error approximately doubles the total error for these analyses. As a consequence, the final measurements from the different experiments, shown in figure 4, differ by less than $1\,\sigma$. For EEC, the correlation between the different measurements, implied by the small scatter in figure 4, is therefore due to their common renormalization scale dependence: an improvement in this situation probably requires a 3rd order calculation.

## The Running of $\alpha_S$

The measurement of $\alpha_S$ at a single energy is, by itself, not a test of QCD: instead QCD predicts the energy evolution of $\alpha_S$. Figure 5 (a) shows the 3-jet event rate $R_3$ measured by the four LEP experiments, in comparison to measurements of $R_3$ from PEP, PETRA and TRISTAN. In all cases the same definition of jets is used. It is seen that $R_3$ is smaller for

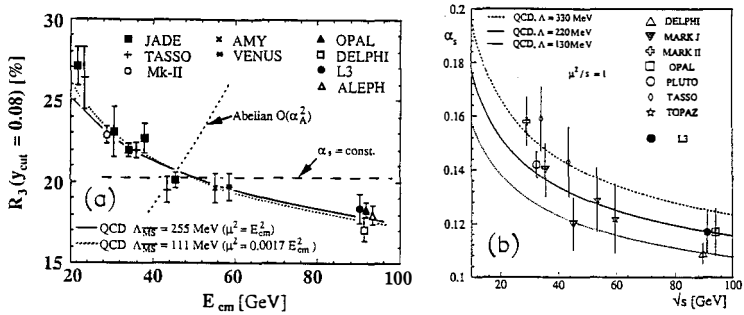


Figure 5: The running of $\alpha_S$ from (a) jet rates (from [8]) and (b) AEEC (from [12]).

the larger energies. In QCD, this decrease in $R_3$ as c.m. energy increases is explained by the "running" of the coupling constant: $\alpha_S$ becomes smaller as $E_{c.m.}$ increases, leading to a smaller rate for hard, acolinear gluon bremsstrahlung and for 3-jet events. The solid and dotted curves in figure 5 (a) show that the data are well described by the 2nd order theory. A similar result is obtained using $\alpha_S$ measurements from the energy-energy correlation asymmetry, shown in figure 5 (b). This running of $\alpha_S$ with energy provides the most direct experimental evidence to date for asymptotic freedom and for non-Abelian structure as predicted by QCD.

## Flavor Independence of $\alpha_S$

L3 has preliminary results [14] setting a limit on the quark flavor dependence of $\alpha_S$. Bottom $b$ quark events are identified through observation of semi-leptonic decays $b \to \mu X$. From a comparison of the 3-jet rate from this $b$-tagged sample to the 3-jet rate from the full multihadronic sample, the result

$$\frac{\alpha_S^b}{\alpha_S^{udsc}} = 1.08 \pm 0.09 \qquad (3)$$

is extracted for the ratio of $\alpha_S$ from $b$ quarks to that from $u$, $d$, $s$ and $c$ quarks; the $\alpha_S$ values for these last 4 quark types are assumed to be equal. The result (3) has been corrected for hadronization and $b$ quark mass effects. The error includes statistical and systematic terms. This result, unique at LEP, places a much more stringent limit on the flavor dependence of $\alpha_S$ than earlier results.

## Inclusive Particle Energy Spectra and Soft Gluon Coherence

OPAL [15] and L3 [16] have studied soft gluon coherence, using inclusive particle energy spectra. In QCD, gluons are emitted coherently, that is by a system of partons instead of by a parton in isolation. This coherence, equivalent to destructive interference, reduces the multiplicity of soft gluons relative the case of no coherence. Figure 6 shows the inclusive charged particle and neutral pion spectra from OPAL and L3, respectively, in terms of the variable $\xi = ln(1/x_p)$, where $x_p = 2 \cdot p/E_{c.m.}$ is the scaled momentum value of the particles. The $\pi^0$ data are the first cross section measurements to be published from LEP for an identified hadron species. Shown in comparison to the LEP data are lower energy measurements. The predictions of analytic formulae based on MLLA calculations, which include coherence, are included as the solid or dotted curves. The comparison of these parton level calculations to the hadron level measurements is justified by local parton hadron duality, which states that the energy and angular distributions of hadrons should closely follow those of the underlying soft gluons. The distributions in figure 6 all exhibit a peak as they approach larger $\xi$ (smaller

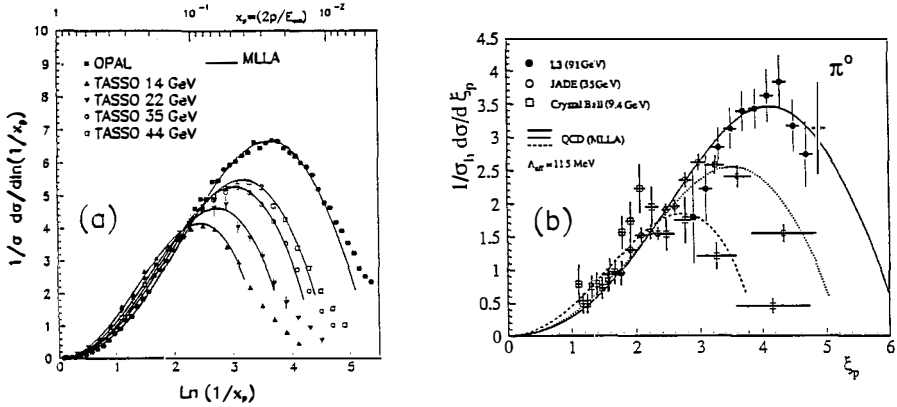


Figure 6: $\xi = ln(1/x_p)$ for (a) charged particles from OPAL [15] and (b) $\pi^0$ from L3 [16].

energy) values and then falloff sharply, for both data and theory. For the MLLA formulae, this falloff is the manifestation of coherence: were the interference not present, the region of large $ln(1/x_p)$ would be more highly populated by soft gluons and there would not be such a falloff. The parameters of the theory have been fit to the LEP data: this yields an unique prediction for the position and shape of the peak in $ln(1/x_p)$ for the other c.m. energy data. The data are in good general agreement with the theory for all c.m. energies, supporting the conjectures of coherence and local parton hadron duality.

## Charged Particle Multiplicity Distribution

DELPHI [17] has published a study of the charged particle multiplicity distribution, including a detailed comparison of LEP data with lower energy $e^+e^-$ measurements. The mean charged multiplicity values $< n_{ch} >$ for $e^+e^-$ experiments above the $\Upsilon$ region are found to fit well with the energy evolution predicted by MLLA analytic formulae, up to the $Z^0$ energy: this can be interpreted as a test of soft gluon coherence and local parton hadron duality in the sense discussed above. DELPHI finds the shape of the charged multiplicity distribution in $e^+e^-$ annihilations, expressed in terms of the variable $z = n_{ch}/ < n_{ch} >$, to be essentially the same for all c.m. energies between 14 and 91 GeV: this "KNO scaling" implies that the underlying dynamics are based on multiplicative branchings [18], providing a statistical test of the QCD framework for multiparticle production through a parton cascade.

## The String Effect

A study of the population asymmetry between jets in 3-jet events, known as the "string effect," has been published by OPAL [19]. The highest energy jet in the 3-jet events for this study is assumed to be a quark jet $q$ because the gluon jet $g$, as the radiated entity, rarely has the highest energy in $e^+e^- \rightarrow q\bar{q}g$ events. Of the two lower energy jets, one is required to have an electron $e$ or muon $\mu$ track candidate: this $e$ or $\mu$ is assumed to come from a semi-leptonic charm or bottom quark decay and so identifies the jet as being a quark jet (this could also be an antiquark jet $\bar{q}$: there is no distinction between $q$ and $\bar{q}$ in this analysis). The remaining jet is the gluon jet. Use of the lepton tag to identify the two lower energy jets allows events with a symmetric topology to be studied, for which the angle $\psi_{q\bar{q}}$ between the the two quark jets is the same as the angle $\psi_{qg}$ between the high energy quark and the gluon jet. Because of this geometric symmetry, the particle populations between the jets can be compared in a simple and model independent way.

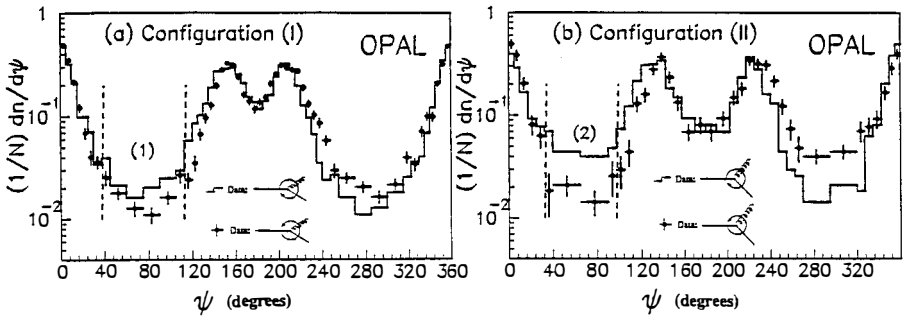


Figure 7: String effect from OPAL [19].

As an example of the OPAL results, figure 7 (a) shows the inclusive multiplicity distribution $(1/N)\, dn/d\psi$ with respect to the azimuthal angle $\psi$ in the 3-jet event plane, for an event sample in which the angles between jets are $\psi_{q\bar{q}} = 150°$ and $\psi_{qg} = 150°$. In the interval enclosed by dashed lines and labeled (1), the region between the higher energy quark jet and the gluon jet is shown by the histogram while the region between the quark and antiquark jets is shown by the points with errors. The histogram lies above the points with errors in this interval: thus the particle population between the $q$ and $g$ is larger than that between the $q$ and $\bar{q}$. A second example is given in figure 7 (b) for a different event sample in which the angles between jets are $\psi_{q\bar{q}} = 130°$ and $\psi_{qg} = 130°$: again the histogram ($qg$ region) lies above the points with errors ($q\bar{q}$ region) in the region between jets, labeled (2) in figure 7 (b). OPAL has verified that these measurements are not strongly affected by the requirement of the lepton tag: thus these asymmetries in particle population cannot be of kinematic origin, due to the geometric symmetry in the events. This analysis establishes that dynamical differences exist between quarks and gluons or between $q\bar{q}$ and $qg$ systems, with respect to their particle production properties.

## Quark-Gluon Jet Differences

A related study to the string effect one, this one preliminary, has also been performed by OPAL [20]. This analysis makes use of the 3-jet event sample selected for the string effect, discussed above, but concentrates on the jet peaks instead of the regions between jets. Figure 8 shows the ratio of the scaled particle energy spectrum from the core region of the gluon jets to that from the core region of the lower energy quark jets, for the event sample shown in figure 7 (a). The jet core region is defined by $135° < \psi < 165°$. The particle energies are scaled by the energy of the jet $E_{jet}$ to which they belong. Since the gluon and lower energy quark jets in this sample have the same energy and event environment, as required by the event selection, their properties can be compared directly. The particle energy spectrum from the gluon jet is observed to be softer than that from the quark jet. OPAL finds that this observation is not affected in a significant way by the lepton tag requirement: a Monte Carlo study indicates that essentially the same result is obtained regardless of whether the lepton tagged sample or a sample with a normal mixture of quark flavors and hadron decays (on the $Z^0$ peak) is used. This is seen by comparing the dashed and solid histograms in figure 8. From an analogous study, gluon jets are found to have a larger angular width than quark jets. These observations agree with the expectations from QCD for the difference between quark and gluon jet structure.

## References

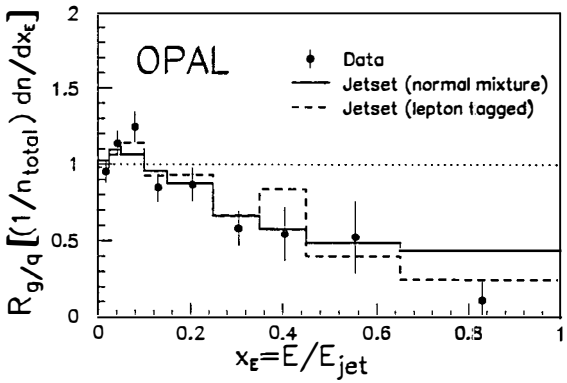


Figure 8: Quark-gluon jet differences from OPAL [20].


1. DELPHI Collab., P. Aarnio *et al.*, Phys. Lett. **240B** (1990) 271.
2. S. Brandt *et al.*, Phys. Lett. **12** (1964) 57; E. Fahri, Phys. Rev. Lett. **39** (1977) 1587.
3. T. Sjöstrand, Comp. Phys. Comm. **39** (1986) 347; T. Sjöstrand and M. Bengtsson, Comp. Phys. Comm. **43** (1987) 367.
4. G. Marchesini and B.R. Webber, Nucl.Phys. **B310** (1988) 461.
5. OPAL Collab., M. Z. Akrawy *et al.*, Z. Phys. **C47** (1990) 505.
6. N. Magnoli, P. Nason and R. Rattazzi, Phys. Lett. **B252** (1990) 271.
7. OPAL Collab., M. Z. Akrawy *et al.*, Phys. Lett. **B235** (1990) 389.
8. S. Bethke, CERN-PPE/91-36, Proc. Workshop on Jet Physics at LEP and HERA, Durham England (Dec. 1990).
9. Z. Kunszt *et al.*, Z Physics at LEP 1, CERN-89-08 (1989).
10. C.L. Basham *et al.*, Phys. Rev. Lett. **41** (1978) 1585; Phys.Rev. **D17** (1978) 2298.
11. ALEPH Collab., D. Decamp *et al.*, Phys. Lett. **B257** (1991) 479.
12. L3 Collab., B. Adeva *et al.*, Phys. Lett. **B257** (1991) 469.
13. OPAL Collab., M. Z. Akrawy *et al.*, Phys. Lett. **B252** (1990) 159.
14. S. Banerjee, XXVIth Rencontres de Moriond, High Energy Hadronic Interactions, Les Arcs, France (1991).
15. OPAL Collab., M. Z. Akrawy *et al.*, Phys. Lett. **B247** (1990) 617.
16. L3 Collab., B. Adeva *et al.*, Phys. Lett. **B259** (1991) 199.
17. DELPHI Collab., P. Abreu *et al.*, CERN-PPE/90-173.
18. R. Szwed, G. Wrochna and A. K. Wroblewski, Mod. Phys. Lett. **A6** (1991) 245.
19. OPAL Collab., M. Z. Akrawy *et al.*, CERN-PPE/91-31.
20. N. Geddes, XXVIth Rencontres de Moriond, High Energy Hadronic Interactions, Les Arcs, France (1991).